Journal of the European Ceramic Society **13** (1994) 427–436

High Temperature Fracture of a SiC Whisker-Reinforced Alumina in Air and Vacuum

T. Hansson,[a] A. H. Swan[b] & R. Warren[a]*

[a] Department of Engineering Metals,
[b] Department of Physics, Chalmers University of Technology, S-412 96 Gothenburg, Sweden

(Received 24 August 1993; accepted 26 November 1993)

Abstract

The fracture behaviour of a SiC_w/alumina composite was studied between room temperature and 1320°C in vacuum by four-point bend testing of specimens pre-cracked by bridge indentation. The results are compared to those of earlier work on a similar material in air. In vacuum, the composite begins to exhibit stable crack growth (SCG) and increasing apparent toughness at about 1100°C. Between 1100 and 1320°C, the extent of SCG increases and the toughness rises to almost three times the room temperature fracture toughness. The toughness enhancement is due mainly to such processes as crack deflection, crack branching, microcrack zone formation and crack tip blunting rather than any temperature-related increase in intrinsic fracture resistance of the material. In air, the fracture processes are similar to those in vacuum but the toughness increase is delayed by about 100°C and the level of toughening is lower. These differences arise from the formation of a glass phase in air which delays microcrack formation but reduces the resistance to stable crack growth.

Das Bruchverhalten eines SiC_w/Aluminiumoxid-verbundes wurde bei Raumtemperatur und bei 1320°C im Vakuum an Vierpunktbiegeproben mit Anriß untersucht. Die Rißeinleitung erfolgte mittels eines Brückeneindrucks. Die Ergebnisse wurden mit früheren Untersuchungen, die in Luftatmosphäre durchgeführt wurden, verglichen. Im Vakuum zeigten die Verbunde ein stabiles Rißwachstum (SCG) und eine zunehmende, scheinbare Zähigkeit bei etwa 1100°C. Zwischen 1100 und 1320°C nimmt das SCG weiter zu und die Zähigkeit steigt auf einen dreimal so hohen Wert wie er bei Raumtemperatur gemessen wird. Die Zähigkeitszunahme wird hauptsächlich durch folgende Prozesse verursacht: Rißablenkung, Rißverzweigung, die Bildung einer Mikrorißzone und die Abstumpfung des Risses und wird nicht durch eine temperaturabhängige Zunahme des materialspezifischen Bruchwiderstandes verursacht. In Luftatmosphäre sind die Bruchvorgänge ähnlich wie im Vakuum, aber die Zähigkeitszunahme ist um etwa 100°C verzögert und die Zunahme ist kleiner. Der Unterschied wird durch die Bildung einer Glasphase an Luft hervorgerufen, die die Bildung der Mikrorißzone verzögert, aber ein stabiles Rißwachstum begünstigt.

Le comportement à la fracture d'un composite alumine/trichite en SiC a été étudié sous vide de la température ambiante jusqu'à 1320°C, à partir d'éprouvettes SEPB soumises à la flexion en 4 points. Les résultats sont comparés à ceux issus de travaux précédents menés sous air sur un matériau analogue. Sous vide, le composite commence à manifester un effet de propagation sous critique et une augmentation de la ténacité apparente autour de 1100°C. Entre 1100 et 1320°C, l'étendue de la propagation sous critique devient plus importante et la valeur de la ténacité augmente pour valoir pratiquement trois fois celle obtenue à température ambiante. L'augmentation de ténacité est principalement due à des mécanismes tels que la déviation et le branchement de fissure, la formation d'une zone microfissurée et de l'émoussement en front de fissure plutôt qu'à tout phénomène d'augmentation de la résistance intrinsèque la fracture du matériau tributaire de la température. Sous air, les processus qui contrôlent la fracture sont analogues à ceux observés sous vide mais, l'augmentation de ténacité est retardé d'environ 100°C et le niveau de renforcement est plus faible. Ces différences sont imputables à la formation d'une phase vitreuse sous air qui

* Present address: Division of Engineering Materials, Luleå University, S-971 87 Luleå.

Journal of the European Ceramic Society 0955-2219/94/$7.00 © 1994 Elsevier Science Limited, England. Printed in Great Britain

retarde la formation de microfissures mais réduit la résistance à la propagation stable.

1 Introduction

It is now well-established that SiC whiskers in SiC_w/alumina composites impart a significant improvement to the fracture toughness (K_{IC})[1-4] and under certain circumstances improvements in creep resistance.[5-9] Although the fracture behaviour of such composites has been studied extensively both at room temperature and elevated temperatures, there is still considerable controversy regarding the mechanisms of toughening. Proposed toughening mechanisms include whisker bridging, pull-out, microcracking, deflection and change of fracture mode from inter- to transgranular. One reason for this apparent disagreement is the fact that ostensibly similar materials from different sources can behave differently, largely because of differences in the whisker/matrix interface. This work is restricted to a commercially-available material from one source containing 33 vol.% whiskers and prepared by hot pressing.

A number of studies[2,3,10] have shown that up to about 1200°C (in air) this material behaves in a linear elastic manner with little indication of *R*-curve behaviour. The mean fracture toughness, K_{IC}, varies between 5 and 8 MPa$\sqrt{m}$ depending on measuring technique, degree of whisker agglomeration, crack orientation and crack propagation direction with respect to the hot pressing direction.[3] Hansson *et al.*[3] have proposed that the toughening at room temperature is largely the result of a change in fracture mode in the matrix from intergranular to transgranular brought about by the presence of the whiskers.

Between 1200°C and 1300°C in air, an apparent increase in toughness occurs associated with microcracking ahead of the crack tip, sub-critical crack growth (SCCG; hereafter in this work it is considered more appropriate to refer to this as stable crack growth, SCG) and crack branching. It has been proposed that the toughening in this case is due to an increase in crack deflection and/or branching as SCG proceeds[2] and/or interaction between the main crack and the microcracks.[10] From around 1400°C the toughness apparently falls again. This seems to be the result of a rapid increase in microcracking and cavitation (i.e. microstructural degradation) associated with the formation of increasing amounts of glassy phase in the microstructure due to oxidation.[10]

The present work was undertaken to throw further light on the elevated temperature fracture processes by performing studies similar to the above but in vacuum rather than in air. Above all, this would have the effect of minimising the formation of the glassy phase. The basis of the study was the examination of fracture initiated from sharp pre-cracks under four-point bend loading. This technique not only provides fracture toughness values in the lower temperature range, but also has the advantage of confining high-temperature deformation and failure processes to the crack-tip region thus permitting well-defined metallographic studies. A further extension of this technique, described previously by Han *et al.*,[2,10] was also exploited here, namely, crack-tip process zones, developed at elevated temperatures, are frozen in before final fracture by cooling the specimen slowly to room temperature. After metallographic examination the specimen can be fractured at room temperature to provide an assessment of the apparent toughness increase caused by the crack and microcrack configurations generated at temperature.

2 Experimental Procedure

2.1 Experimental overview

Parallel studies to those in air described above were performed on the same material but in a vacuum of approximately 4×10^{-5} torr. In both cases tests were performed on single edge pre-cracked bars loaded in four-point bending. The pre-cracks were created by different methods in the two studies; in the air tests they were generated from sawn notches by cyclic compression fatigue[10] while in the present work they were created by bridge indentation.[3] This difference, however, is not considered to be significant since little or no wake-related toughening is expected to occur in this material. The matrix grain size, around 2 μm, is too small to give significant grain bridging and any whisker bridging would be confined to a region close to the crack tip.[11]

The following experimental studies were made:

(i) Conventional fracture toughness measurements were made between room temperature and 1320°C. Above 1000°C where stable crack growth occurred, the growth was estimated by observation of the fracture surface and side profiles.

(ii) Selected specimens were subjected to constant loads at 1270°C, first to generate crack-tip process zones to be frozen in by cooling for subsequent study and fracture at room temperature, and secondly to assess the nature and degree of time-dependent deformation (creep) occurring at

temperature. A similar creep experiment was carried out in air in the earlier study.[2]

(iii) A specimen loaded sub-critically but close to fracture at 1320°C was cooled and the crack-tip region was examined with scanning and transmission electron microscopy, as were the as-received microstructure and the tip region of an untested precrack.

Wherever possible the results of these studies are compared to those obtained in air.

2.2 Material

The composite chosen for this study was a commercially available material (WG 300, Greenleaf Co., Saegertown, PA) containing 33 vol.% SiC whiskers in α-alumina. Following a proprietary powder blending process, the alumina/whisker mixture is uniaxially hot pressed in the form of plates to practically full density. The material is of high purity and generally exhibits little or no glassy phases at grain boundaries while the whisker/matrix interfaces exhibit a thin (<10 nm) amorphous film.[8] The whiskers have diameters largely between 0·1 and 1 μm and aspect ratios of 10–100. The alumina grain size is 1–2 μm. Further details of the material are given by Han *et al.*[10]

2.3 Fracture tests

All tests in this study were performed in vacuum on single edge pre-cracked bend-bars in four-point bending. The bend-bars had dimensions ($B \times W \times L$) of 3 × 6 × 45 mm or 4 × 8 × 45 mm and the bending unit had inner and outer spans of 19 and 38 mm respectively. To examine the microstructure and measure the pre-crack lengths the samples were polished on the side surfaces. The top and bottom surfaces were ground parallel to each other to within 0·01 mm in order to minimise twisting of the samples during tests. Pre-cracks were produced by bridge indentation as described by Hansson *et al.*[3] Pre-crack lengths varied between 2 and 4 mm. These details should be compared to those of the studies in air[10] which employed specimens with dimensions 5 × 10 × 50 mm and a sawn notch depth of 3·2 mm with additional fatigued pre-crack lengths of up to about 200 μm. The bend-rig spans in this case were 20 and 40 mm.

The fracture toughness and creep tests in vacuum were performed in a screw driven electromechanical testing machine (Instron 8562) using a four-point bend-rig of SiC specially designed to avoid twisting of the samples during tests.[3] The toughness tests were performed at a crosshead speed of 1 μm/s while the creep samples were loaded, after attainment of the test temperature, at a rate of 0·3 N/s. The tests in air were carried out in a hydraulic machine at a rate of 0·5 μm/s and it was possible to view the crack on one side of the specimen using an optical system with 40× magnification.[10]

The vacuum chamber, incorporating a resistance furnace, load cell and device for measuring sample deflection, was fitted beneath the crosshead. This system was limited to a maximum temperature of around 1320°C. Samples from those tests that were interrupted before fracture were used to determine residual deflection, crack extension and crack morphology as well as fracture toughness at room temperature.

At high temperatures stable crack growth and crack tip processes can lead to deviations from ideal crack geometry. It is therefore important to note that here, stress intensities and corresponding fracture toughnesses were defined on the basis of nominally ideal, mode I geometries. Thus, fracture toughness was defined in two different ways: (i) a nominal toughness, denoted K_{IC}, was calculated using maximum load and the initial pre-crack length; (ii) an apparent value, here termed K^*_{IC}, was calculated using the total crack length (i.e. including stable crack growth estimated to have existed at the initiation of unstable fracture and the fracture load at that point. The total crack length was estimated by adding the original crack length and stable crack growth measured on the fracture surfaces and side surfaces. The apparent toughness as defined here takes into account stable growth but neglects any associated deviation from ideality.

2.4 Electron microscopy

Fracture surfaces and polished sections of pre-cracked and bend tested specimens were examined using SEM (CamScan S-4 80 DV). For more detailed examination requiring higher resolution, transmission electron microscopy (TEM) was used. The TEM specimens were taken from as received material and from the crack tip regions of an unloaded pre-cracked sample and a sample tested at 1320°C but unloaded just prior to failure. In the latter two samples the circular TEM specimen was centred close to the crack tip. The specimens were dimple ground followed by ion beam thinning. TEM examination was carried out on a JEOL 2000FX 200kV TEM/STEM microscope.

3 Results

3.1 Fracture toughness versus temperature

Figure 1 shows the nominal fracture toughness in air[10] and vacuum as a function of temperature up to 1400°C. As indicated above the nominal fracture

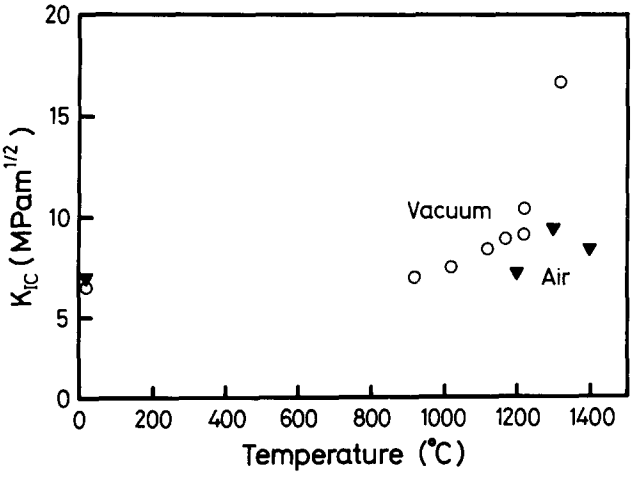

Fig. 1. The effect of temperature on the nominal toughness of the composite tested in air and vacuum.

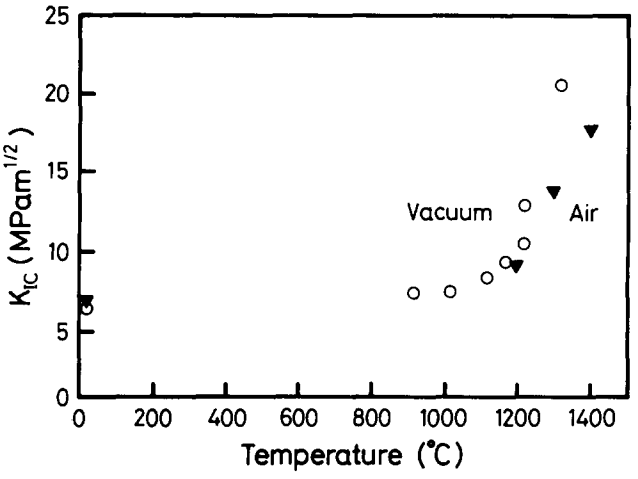

Fig. 2. The effect of temperature on the apparent toughness of the composite tested in air and vacuum.

toughness values are derived using the original pre-crack length and maximum load. In vacuum the material shows a monotonically increasing fracture toughness with temperature up to 1320°C. In air the nominal fracture toughness increases with temperature up to 1350°C and decreases with further increases in temperature above 1350°C. The increase in fracture toughness in vacuum is more pronounced and starts at a lower temperature than in air.

Further insight as to the effect of the two environments is gained by considering the apparent fracture toughness (K^*_{IC}) based on the total crack length and load at the point of fast fracture initiation (see Fig. 2). The differences between the behaviour in air and in vacuum are now less obvious. Up to 1300°C the general trends are similar to those for the nominal toughness described above, but above 1300°C the apparent toughness in air does not decrease but continues to rise. The reason for this apparent difference in results is that for a given temperature the stable crack growth that had occurred at the point of failure was more extensive in air than in vacuum (which means that for fracture in air the nominal K_I values underestimate the true value to a greater extent). This can be seen by comparing the pre-crack and total crack lengths summarised in Table 1.

An example of stable crack growth is shown at low magnification in Fig. 3. This shows that the growth was accompanied by significant crack branching. Such branching was typical both in air and vacuum at 1300°C and above. At lower tem-

Table 1. Crack lengths and fracture toughness values

Temperature (°C)	*Pre-Crack length (mm)*	*Total crack length at fracture (mm)*	K_{IC} *(MPa√m)*	K^*_{IC} *(MPa√m)*
Vacuum				
20	—	—	6·5[a]	6·5[a]
920	3·16	3·34	7·0	7·5
1 020	2·98	3·03	7·5	7·6
1 120	3·84	3·86	8·4	8·5
1 170	4·09	4·25	8·9	9·5
1 220	2·40	2·90	9·1	10·6
1 220	2·76	3·45	10·4	13·0
1 320	3·39	3·96	16·7	20·6
Air				
20	3·35	3·35	7·0	7·0
1 200	3·29	4·30	7·2	9·3
1 300	3·28	4·58	9·4	13·9
1 400	3·30	6·25	8·4	17·8

[a] Average of four measurements.

Fig. 3. Optical micrograph of a crack in a testbar loaded to K^*_{IC} = 15 MPa√m in vacuum at 1320°C and unloaded before final failure. The overall appearance of the crack, dominated by crack branching and microcracks is shown.

Table 2. Summary of interrupted tests and constant load creep experiments

No.	*Temp. (°C)*	*Pre crack length (mm)*	*SCG (mm)*	*Retained defln (μm)*	*Loading conditions (MPa√m) (μm)*	K^*_{IC} *after test (MPa√m)*	*Comments*
Vacuum							
I.1	1 320	3·50	0·33	53	K_I = 5·8 (0·9$K_{IC,RT}$) 0 min	10·6	Interrupted test K_{IC} measured at RT. Loading rate 1 μm/s
I.2	1 320	1·79	0·66	37	K_I = 12·1 (1·86$K_{IC,RT}$) 0 min	n.d.	K^*_I = 15·0 when interrupted. Loading rate 1 μm/s
C1	1 270	2·04	1·76	—	K_I = 6·7 (1·03 $K_{IC,RT}$) 20 min to fracture	16·5	Fracture at 1270°C
C2	1 270	2·94	0·25	49	K_I = 4·5 (0·7$K_{IC,RT}$) 42 min + K_I = 5·3 (0·8 $K_{IC,RT}$) 3 min	10·5	Interrupted test K_{IC} measured at RT
C3	1 270	2·78	1·27	155	K_I = 5·4 (0·7$K_{IC,RT}$) 1 h	18·9	Interrupted test K_{IC} measured at RT
C4	1 270	3·28	1·12	—	K_I = 8·1 (1·03 $K_{IC,RT}$) 40 s to fracture	16·5	Fracture at 1270°C
Air							
C5	1 300	3·20	0·80	15	K_I = 8·2 (1·17 $K_{IC,RT}$) + stress relaxation 190 s + K_I = 6·2 (0·89 $K_{IC,RT}$) 36 min	n.d.	Load fell from 1210 to 900 N during stress relaxation

peratures crack branching was relatively rare but the stable growth exhibited considerable deflection.

A general observation is that the apparent toughness, K^*_{IC}, increases with the length of stable crack growth, the increase per unit crack extension being greater in vacuum than in air.

3.2 Interrupted tests and creep tests

In order to gain further insight regarding the effect of crack morphology on the fracture toughness of the material, different crack configurations were created by interrupted loading at temperature and by creep crack growth at constant load. Subsequent fracture toughness tests were carried out either at room temperature after examination of the crack or directly at the creep température. Table 2 gives details of the tests and, where appropriate, corresponding fracture toughness values. Loads are given in terms of the nominal stress intensities at the original pre-cracks. Since the test bars (I.2, I.2, C1, C2), (C3, C4) and C5 were taken from three different batches of material with slightly different room temperature toughnesses, the loads are also quoted as fractions of the room temperature toughness.

Two types of creep test were carried out in vacuum; the first involved loading to a stress intensity just above the room temperature fracture toughness and allowing the creep crack growth to proceed to fracture, while in the second, loading was to 70–80% of the room temperature toughness and the test was interrupted before fracture. In the latter, the permanent bend deflection retained after the test was measured before subjecting the sample to a room temperature fracture toughness test. The test in air was similar to the second type of test except that this was preceded by a short stress-relaxation experiment of 190 s duration. This specimen was not fractured but used for TEM studies of the crack tip region. The two tests I.1 and I.2 were interrupted rising load tests; I.2 was interrupted as close as possible to the final fracture and used for TEM examination.

A general conclusion of these tests is that all specimens exhibited stable crack growth with branching. It is found that the average growth rates increased systematically with the applied stress intensity (rather than the normalised value). Assuming a power law dependence of growth rate on K_I the exponent lies between 10 and 20. The growth rate in air is also consistent with this. The degree of crack branching increased with the crack growth and a clear relationship between the extent of growth and the associated apparent toughness was observed (cf, the similar observation in the fracture toughness tests described in the previous section). Thus, specimens exhibiting comparable levels of crack growth (e.g. C1, C3 and C4 or I.1 and C2) had similar values of apparent fracture toughness regardless of their loading history.

Table 3. Elevated temperature crack development followed by room temperature fracture toughness testing

	Vacuum			*Air*			
Specimen	C2	C3	I1	A1	A2	A3	A4
Temp. (°C)	1270	1270	1320	1300	1300	1300	1400
Initial crack length, a_o (mm)	2·94	2·78	3·50	3·29	3·42	3·37	3·3
Stable crack growth (mm)	0·25	1·27	0·33	~0·1	~0·5	~0·1	2·95
Nominal fracture toughness K_{IC} (MPa$\sqrt{m}$)	9·2	9·1	8·6	7·6	9·1	9·1	8·4
Apparent fracture toughness K^*_{IC}(MPa$\sqrt{m}$)	10·5	18·9	10·6	8·0	11·3	8·9	14·4
Predicted toughening by branching	×1·53	×1·51	×1·50				
Observed toughening	×1·61	×2·40	×1·63				
Perm. bend defl. (μm)	49	155	53	≈0	≈0	≈0	85
Comments	Branching	Branching microcrack zone	Branching	Deflection	Branching	Deflection	As C3

The retained bend deflection in interrupted tests revealed that significant permanent crack tip deformation had occurred. This was greater in vacuum than in air. In vacuum significant permanent deformation was even observed in the rising load tests whereas in air no such deformation could be detected in such short times at 1300°C[3] (see also Table 3).

Samples C1 and C4 loaded at high stress intensity until fracture at temperature both exhibited similar extensive stable crack growth (with branching) resulting in the same apparent fracture toughness (16·5 MPa$\sqrt{m}$), more than double the room temperature value. It should be noted that in specimen C1 limited instantaneous crack growth had occurred already during loading at a stress intensity of 6·2 MPa$\sqrt{m}$ ($0{\cdot}95K_{IC,RT}$). This crack growth was indicated by a drop in load and increased bend deflection followed by a marked increase in compliance.

Specimens C2 and C3, loaded at lower stress intensity, were submitted to different holding times in order to generate different degrees of development of crack morphology. This demonstrated that crack growth, permanent deformation and the degree of branching increased with time producing corresponding increases in apparent fracture toughness (measured at room temperature). In specimen C3 the crack branching had developed into a crack tip zone of extensive microcracking about 1 mm in diameter, easily observable in the optical microscope. This evidently led to the very high room temperature apparent toughness (18·9 MPa$\sqrt{m}$).

The sample loaded in air, C5, exhibited qualitatively similar behaviour to the vacuum tested samples. Optical observation of the sample during the test revealed that stable crack growth began during initial loading when the stress intensity reached about 8·0 MPa$\sqrt{m}$ ($1{\cdot}1K_{IC,RT}$) and continued during stress relaxation until the stress intensity fell below this value. During the subsequent constant load creep at K_I = 6·2 MPa$\sqrt{m}$ no further observable crack growth occurred. Instead a zone of deformation about 250 μm in diameter developed around the newly created crack tip which no doubt accounted for most of the observed 15 μm bend deflection. The TEM investigation confirmed that this zone contained a high level of microcracking.[2] As noted above, the amount of permanent deflection is less than for corresponding conditions in vacuum.

3.3 Room temperature fracture of cracks created at temperature

The nominal and apparent room-temperature fracture toughnesses (K_{IC} and K^*_{IC} respectively) of specimens containing cracks and deformation zones created at high temperature are given in Table 3. Comparison of the fracture toughness values in Table 3 with those in Tables 1 and 2 confirms that the room temperature values lie only slightly lower than corresponding at-temperature values with similar stable crack growth. As already noted, this indicates that the apparent toughening is largely due to the effects of crack geometry which are evidently retained on cooling rather than any temperature-related increases in the intrinsic fracture energy. Also included in Table 3 are estimates of the degree of apparent toughening predicted on the basis of a model of simple crack branching applied to the cracks as observed in the creep specimens.[12] The calculation used was developed for a two dimensional crack with single branching and a 90° angle between the two crack branches. The toughening in specimens

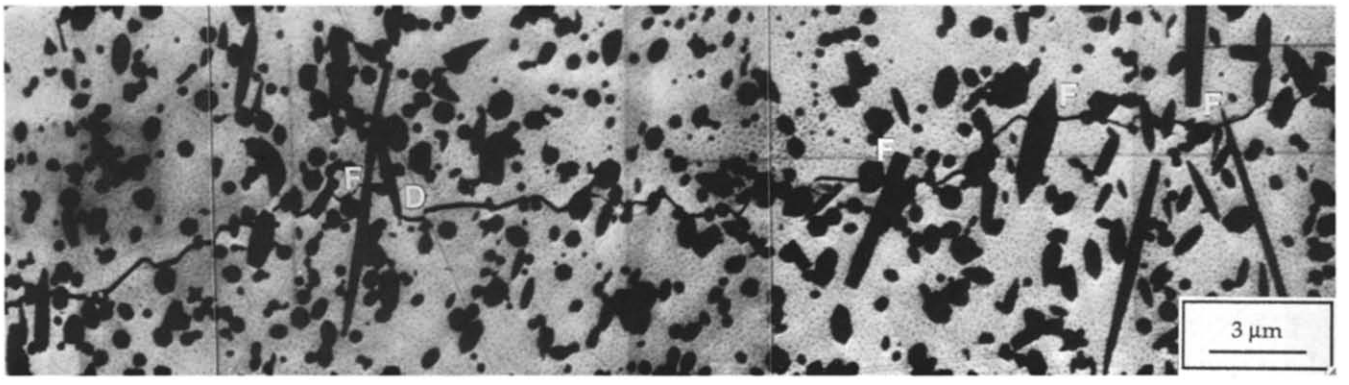

Fig. 4. SEM micrograph of a bridge indentation precrack. The micrograph was taken normal to the crack plane. Whiskers perpendicular to the crack plane have fractured close to the crack plane (F), while the crack is deflected along whisker interfaces for lower angles of incidence (D). No microcracking or crack branching could be observed.

I.1 and C2, which exhibited relatively uncomplicated, branched cracks, is predicted well by the model whereas specimen C3 with a large and heavily microcracked zone exhibits more toughening than predicted.

3.4 Electron Microscopy

A SEM micrograph of a bridge pre-crack is shown in Fig. 4. The micrograph was taken on the side of the sample, i.e. perpendicular to the crack plane and parallel to the crack growth direction. The crack propagated in more or less straight paths through the alumina matrix. Whiskers oriented perpendicular to the crack plane have fractured close to the crack, while for lower angles of incidence the crack is deflected along whisker interfaces. No microcracking or crack branching could be observed. It is also confirmed that in contrast to unreinforced alumina with similar grain size, the matrix fracture at room temperature is predominantly transgranular.

At elevated temperatures the fracture behaviour changed completely, as seen in Figs 3 and 5. The figures show a side section perpendicular to the crack plane in sample I.2 (Table 2) tested in vacuum at 1320°C and interrupted before failure at an apparent stress intensity of 15 MPa$\sqrt{m}$. Figure 3 shows the general appearance of the branching crack, while Fig. 5 is a SEM micrograph of the same specimen. Extensive microcracking and crack branching is observed. The whiskers may aid the microcracking by acting as stress concentration sites ahead of the crack tip causing microcracks to emerge from the whisker ends. Other possible sites for microcracking are whisker/matrix interfaces and matrix grain boundaries. The proportion of intergranular fracture seems to be greater than in the case of room temperature fracture. Nevertheless, transgranular fracture still occurred as was made clearer by TEM. A TEM micrograph from the crack zone of the same sample is shown in Fig. 6. A number of cracks can be seen, propagating from whisker to whisker as in the room temperature pre-crack. However there is more whisker debonding and indications of bridging and pullout in this case. Crack branching is also observed.

In contrast to samples tested under similar conditions in air there is no indication of glass formation beyond the small amount found in the as-received material. Nevertheless, it seems that the interfaces become weaker with temperature.

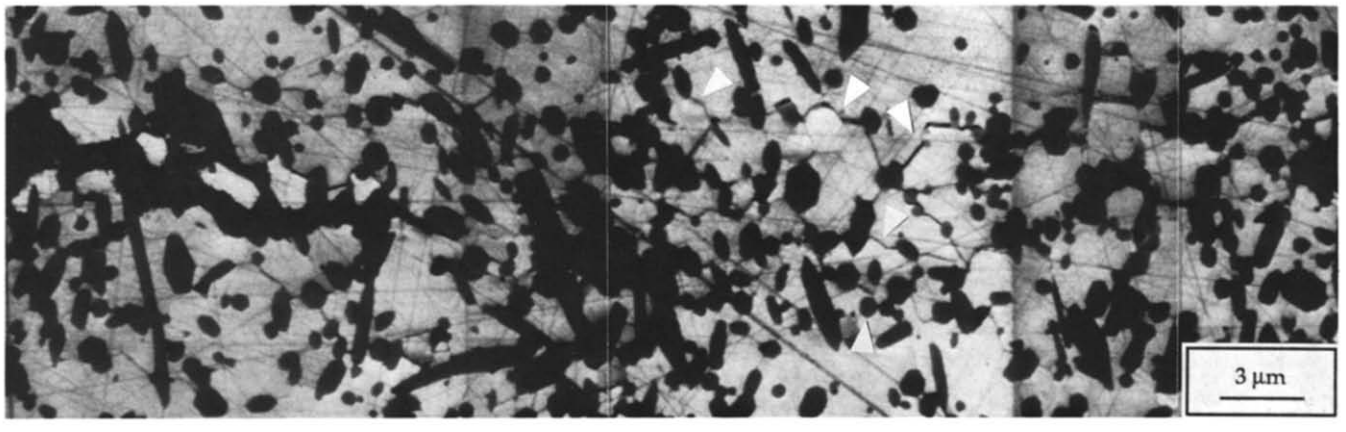

Fig. 5. SEM micrograph showing a section normal to the crack plane in the same sample as Fig. 3. A high density of microcracks and crack branching were observed in this specimen (examples arrowed). There is evidence that whiskers may have encouraged microcracking since microcracks are observed to emerge from whisker ends.

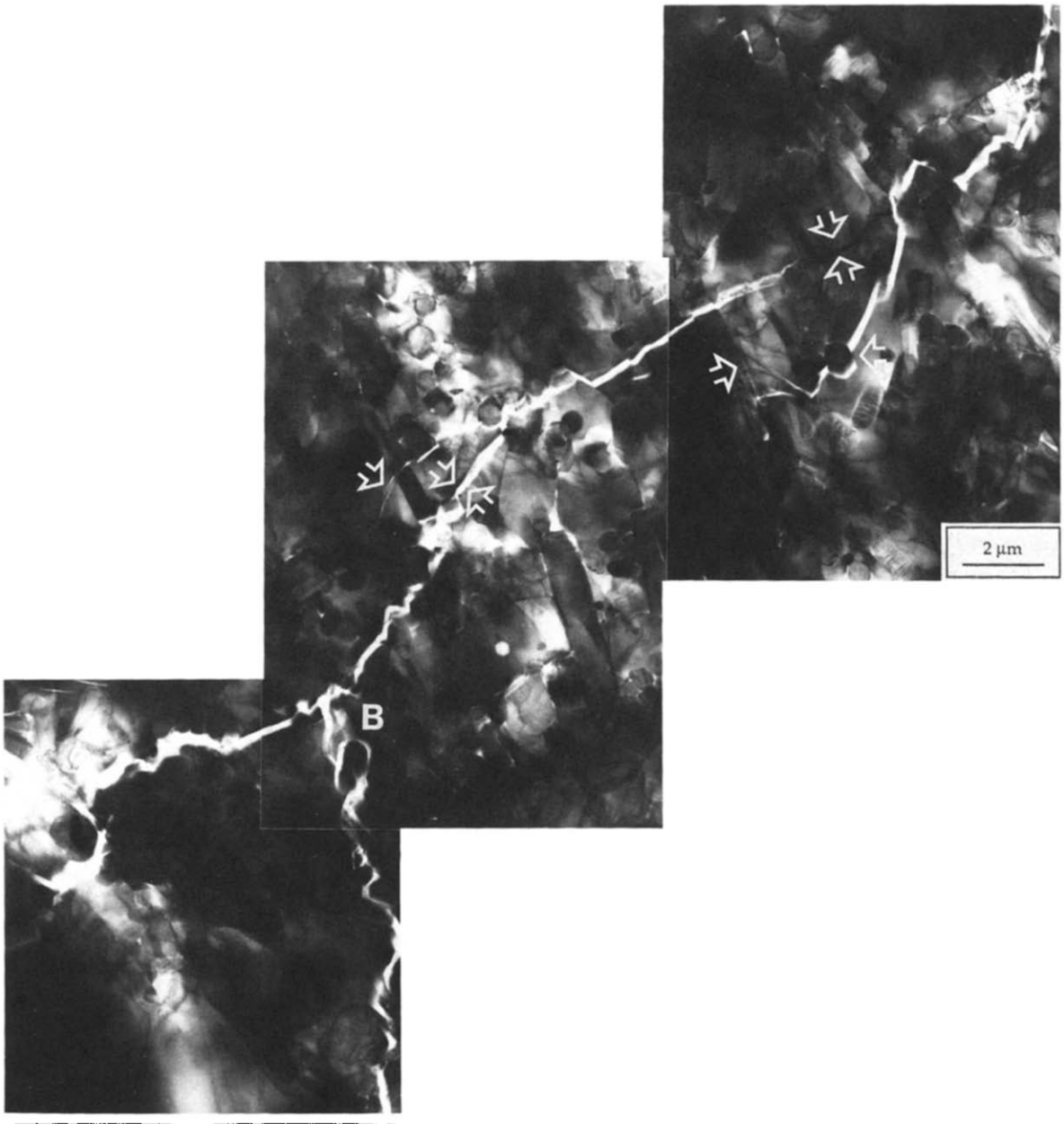

Fig. 6. TEM micrograph from the crack tip region of the sample in Fig. 3, showing several cracks propagating transgranularly between neighbouring whiskers as was observed at room temperature.

Another significant difference is that there appears to be a greater microcrack density in the vacuum-tested sample than was observed in samples tested in air at a similar temperature.[10]

4 Discussion

The observations of fracture behaviour presented above can be discussed and qualitatively explained on the basis of three distinct processes occurring in the crack tip region at high temperature, namely; cavity/microcrack formation, stable crack growth and glass formation. Although these processes are interactive it is important to distinguish between them since they occur in parallel and depend differently on the test parameters stress, temperature and environment.

The cavity and microcrack formation and growth in this composite are stress dependent and thermally activated time-dependent processes associated with diffusion-based deformation and begin to be significant above about 1000°C. At constant loads beneath the critical stress intensity they lead to time-dependent permanent deformation with or without crack growth.

Considering first rising load conditions, it is proposed that stable crack growth initiates when the critical stress intensity for normal unstable room temperature crack growth is reached; the initiated crack is quickly stabilised by crack deflection, crack branching, crack bridging, microcracking or some other shielding process. The observations indicate that this shielding, initially (i.e. in the lower temperature range (1000–1200°C) and in the early stages of growth) might be simply due to

an increased deflection or branching caused by linkage of the main crack with the microcracks. Stable crack growth accompanied by an apparent increase in toughness will therefore commence at a temperature that gives the appropriate microcracking rate at the current stress intensity. With increasing temperature the rate of microcracking and associated permanent deformation increases leading to more extensive crack growth, deflection, branching as well as an increased opportunity for interactions between the main crack and the microcrack zone, processes which in turn lead to increasing apparent toughness.

Under constant load conditions similar phenomena are possible and are observed. However, the rising stress intensity caused by crack growth is at least partly offset by the crack tip shielding and blunting. Thus, it can be predicted that decreasing the initially applied stress intensity will reduce the ratio of crack growth to tip zone development. It can also be understood that below a certain threshold stress intensity the crack will be arrested and give way to general creep deformation.

Sample C3, tested at room temperature after being subjected to a load cycle at 1270°C showed a remarkable 2·4-fold increase in apparent toughness relative to its normal room temperature toughness; even more remarkable is the threefold increase in toughness observed at 1320°C in the rising load test (Table 1). These increases exceed the toughening predicted for crack branching alone. Interaction between microcracks and the main crack probably also contributes to toughening. According to Kachanov *et al.*[13] the contribution is dependent on the microcrack morphology, only certain microcrack morphologies giving a positive toughening; even in the most favourable case the relative toughening due to microcracking is limited to 1·33 which is still insufficient to explain the above values. Additional toughening could originate from bridging between the observed long crack branches. That such bridging occurs was confirmed by examination of both sides of the samples and by SEM examination of fracture surfaces which revealed that the branches did not normally extend through the thickness, but rather formed a treelike network visible as flakes on the fracture surfaces. Another possible source of toughening is crack tip blunting resulting from the creep deformation that evidently occurs in the crack tip zone during loading prior to fracture. Non-elastic deformation around deflected and branched cracks has been treated theoretically for strain hardening material by Suresh and Shih.[14] Similar behaviour can be expected for creep conditions around the crack tip if the creep exponent is substituted for the strain hardening exponent. In general, the stress level (i.e. stress intensity) decreases with increasing creep exponent and angle between the branches. Assuming a creep exponent of around 5,[8] significant contributions to toughening can be expected in these samples.

The metallographic studies and observed retained bend deflection indicated that up to around 1300°C microcracking occurs more readily in vacuum than in air and this is consistent with the fact that the increasing toughness begins about 100°C earlier in vacuum. On the other hand, for a given temperature, stable crack growth is more extensive under rising load conditions in air than in vacuum. These differences can be attributed to the glass formation caused by the reaction of SiC with the alumina and oxygen in the crack tip region in air at high temperature.[2,10] This glass forms at the whisker/matrix interfaces and penetrates the matrix grain boundaries; that is, it may inhibit microcracking by filling the sites of potential microcracks and filling microcracks as they develop. At the same time the glass pockets and films provide weak paths for easy crack extension.[15] Thus, in air, stable cracks can propagate through the microstructure without involving the same degree of microcracking as in vacuum. It is also to be noted that high temperature fracture in vacuum probably involves a greater proportion of transgranular failure than was observed in air.[10]

The glass phase also provides an explanation for the fact that the toughening in air becomes increasingly less effective than in vacuum with increasing temperature above 1300°C. In this higher temperature range, the crack-growth-related toughening processes observed in vacuum, such as branching and microcrack zone formation, occur to a similar extent in air. However, the increasing amount of glass and its falling viscosity must lead to a sharper fall in crack growth resistance than in vacuum.

5 Conclusions

The fracture toughness (K_{IC}) in vacuum of the SiC_w/alumina composite studied here remains relatively constant up to about 1100°C. At this temperature the material begins to exhibit stable crack growth and the apparent toughness (K^*_{IC}) begins to increase, rising to almost three times the room temperature fracture toughness between 1100°C and 1320°C. The degree of toughness enhancement increases with increasing length of stable crack growth and can be attributed to a number of processes associated with this growth that originate in the microcracking that occurs around the growing crack. Thus, between 1100 and 1200°C,

the toughness increase is mainly the result of deflection of the growing crack probably caused by linking of the main crack with microcracks. With increasing temperature and increasing loading time (for example under constant creep loads) the deflection process gives way to progressively increasing crack branching and finally the development of large deformation zones around the crack tip containing high concentrations of microcracks. The above microcrack-related processes are alone insufficient to account for the highest levels of toughness observed. Bridging over crack branches and permanent creep deformation (blunting) of the crack tip also occur and can be assumed to make additional contributions to the toughness. All the above processes produce an apparent toughening by affecting the crack morphology and it is this rather than any temperature-related increase in intrinsic fracture resistance of the material that leads to the toughness increase.

The above temperature-related processes are also observed for fracture in air. However, the increase in toughness is delayed by about 100°C and the degree of toughening is lower. These differences can be attributed to the formation of a glass phase in the composite microstructure by reaction of atmospheric oxygen with the SiC and alumina. By filling grain and interphase boundaries the glass delays microcracking but reduces the resistance to stable crack growth by providing a weak fracture path.

Acknowledgements

The authors acknowledge the financial support of the Swedish Board of Technical Development (NUTEK).

References

1. Wei, G. C. Becher, P. F., Development of SiC-whisker-reinforced ceramics. *Ceram. Bull.*, **64** (1985) 298–304.
2. Han, L. X., Hansson, T., Suresh, S. & Warren, R., High temperature fracture of SiC whisker reinforced alumina. In *Proc. of 5th Scandinavian Symposium on Materials Science*, ed. I. L. H. Hansson & H. Lilholt. DSM, Copenhagen, 1989, pp. 287–94.
3. Hansson, T., Warren, R. & Wasén, J., Fracture toughness anisotropy and toughening mechanisms of a hot-pressed alumina reinforced with SiC-whiskers. *J. Am. Ceram. Soc.*, **76** (1993) 841–8.
4. White, K. W. & Guazzone, L., Elevated-temperature-toughening mechanisms in a SiCW/Al_2O_3 composite. *J. Am. Ceram. Soc.*, **74** (1991) 2280–5.
5. Chokshi, A. H. & Porter, J. R., Creep deformation of an alumina matrix composite reinforced with silicon carbide whiskers. *J. Am. Ceram. Soc.*, **68** (1985) C-144–C-145.
6. Lin, H, T. & Becher, P. F., Creep-behavior of a SiC-whisker-reinforced alumina. *J. Am. Ceram. Soc.*, **73** (1990) 1378–81.
7. Arellano-López, A. R., Cumbrera, F. L., Domínguez-Rodríguez, A., Goretta, K. C. & Routbort, J. L., Compressive creep of SiC-whisker-reinforced Al_2O_3. *J. Am. Ceram. Soc.*, **73** (1990) 1297–300.
8. Lipetzky, P., Nutt, S. R., Koester, D. A. & Davis, R. F., Atmospheric effects on compressive creep of SiC-whisker-reinforced alumina. *J. Am. Ceram. Soc.*, **74** (1991) 1240–7.
9. Swan, A. H., Swain, M. V. & Dunlop, G. L., Compressive creep of SiC whisker reinforced alumina. *J. Eur. Ceram. Soc.*, **10** (1992) 317–26.
10. Han, L. X., Warren, R. & Suresh, S., An experimental study of toughening and degradation due to microcracking in a ceramic composite. *Acta Metall. Mater.*, **40** (1992) 259–74.
11. Becher, P. F., Fuller, E. R. & Angelini, P., Matrix-grain-bridging contributions to the toughness of whisker-reinforced ceramics. *J. Am. Ceram. Soc.*, **74** (1991) 2131–5.
12. Kitagawa, H., Yuuki, R. & Ohira, T., Crack-morphological aspects in fracture mechanics. *Engng Fract. Mech.*, **7** (1975) 515–29.
13. Kachanov, M., Montagut, E. L. E. & Laures, J. P., Mechanics of crack–microcrack-interactions. *Mech. Mater.*, **10** (1990) 59–71.
14. Suresh, S. & Shih, C. F., Plastic near-tip fields for branched cracks. *Int. J. Fract.*, **30** (1986) 237–59.
15. Chan, K. S. & Page, R. A., Creep damage development in structural ceramics. *J. Am. Ceram. Soc.*, **76** (1993) 803–26.